Effect of the preparation technique of Cu-ZSM-5 catalysts on the isothermal oscillatory behavior of nitrous oxide decomposition

Effect of the preparation technique of Cu-ZSM-5 catalysts on the isothermal oscillatory behavior of nitrous oxide decomposition

Marco Armandi[†], Tahrizi Andana[†], Samir Bensaid, Marco Piumetti, Barbara Bonelli, Raffaele Pirone*

Department of Applied Science and Technology, Politecnico di Torino, Corso Duca degli Abruzzi 24, 10129, Turin, Italy

* To whom correspondence should be addressed

[†]Both authors equally contributed to the work.

Tel.: +39-011-0904735; E-mail address: raffaele.pirone@polito.it

Abstract:

A set of Cu-ZSM-5 samples (Si/Al = 25) was synthesized by wetness impregnation, aqueous phase ion exchange and solid-state ion exchange, SSIE. Copper(II) acetate was used as precursor during both wetness impregnation and aqueous phase ion exchange to prepare excessively-exchanged samples (*i.e.* Cu/Al > 1), whereas SSIE was carried out by sublimating copper(I) chloride. Additionally, a Cu-ZSM-5 sample with extremely low Al content (Si/Al = 500) was prepared by impregnation.

The samples were tested in the catalytic decomposition of N_2O, with the aim of studying possible effects of the preparation technique on the isothermal oscillatory behavior of the reaction rate in a series of tests carried out by varying both the temperature and the residence time. The SSIE sample led to a non-oscillating system, whereas the highest Cu content samples prepared by the two aqueous procedures exhibited clear oscillations of the reaction rate. The Cu-ZSM-5 with Si/Al = 500 was quite inactive, but, surprisingly, gave rise to oscillations of both unconverted N_2O and produced O_2 concentrations at the reactor outlet.

A combined IR spectroscopy and H_2-TPR study showed the role of oligomeric Cu_xO_y species with extra-lattice oxygen close to the Al atoms on the observed oscillations. Such species are much more abundant in the samples prepared by either impregnation or ion-exchange, when Cu/Al > 1. In contrast, the sample prepared by SSIE resulted to be rich in Cu^+ isolated species, active for the reaction, but not inducing oscillation.

Keywords: Cu- ZSM-5, nitrous oxide, decomposition, oscillation, impregnation, ion exchange, solid state ion exchange.

1. Introduction

Interest in Cu-substituted zeolites (ZSM-5, Beta, SSZ-13, etc.) is related to their promising properties in DeNOx lean-burn applications [1,2]. Among them, copper-exchanged ZSM-5 exhibits since the early '90s very interesting and incomparable properties, especially in the reaction of direct decomposition of nitric oxide, of which Cu-ZSM-5 is probably the unique existing effective catalyst [3]. However, as is well documented by decades of continuous papers such a catalyst is unable to sustain the practical operating conditions, most of all due to its poor hydrothermal resistance.

Actually, Cu-ZSM-5 shows unique properties in the decomposition of NO, but also very interesting activity in the classical reduction with ammonia (catalyzed at very low temperatures) and in the fascinating alternative of reduction of NOx with unburned hydrocarbons and/or CO. Such a catalyst is also very active in the decomposition of N_2O which is a harmful compound by itself and also the key intermediate of NO decomposition over such a catalyst.

In fact, Nitrous oxide (N_2O) is considered a greenhouse gas, since it lasts approximately 150 years in the atmosphere, it has 310 and 21 times greater warming potential than CO_2 and CH_4, respectively, and it contributes to the destruction of the stratospheric ozone layer. The main anthropogenic sources of N_2O are, *inter alia*, fertilizers, nitric acid, adipic acid, caprolactam and glyoxal production, fossil fuels and biomass combustion, and sewage treatments. As a whole, nitric and adipic acid production plants are considered the largest industrial sources of N_2O emissions, with higher N_2O concentration in tail gas emissions from adipic acid plants (usually 20 – 40 v/v %) than from nitric acid production (around 300–3500 ppm). Indeed, it has been reported that around 10 % of N_2O yearly released into the atmosphere originates from adipic acid production, and therefore much efforts have been made to abate the N_2O deriving from such source.

In effect, nitrous oxide (N_2O) is considered a greenhouse gas, since it lasts approximately 150 years in the atmosphere, it has 310 and 21 times greater warming potential than CO_2 and CH_4, respectively, and it contributes to the destruction of the stratospheric ozone layer. The main anthropogenic sources of N_2O are, *inter alia*, fertilizers, nitric acid, adipic acid, caprolactam and glyoxal production, fossil fuels and biomass combustion, and sewage treatments. As a whole, nitric and adipic acid production plants are considered the largest industrial sources of N_2O emissions, with higher N_2O concentration in tail gas emissions from adipic acid plants (usually 20 – 40 v/v %) than from nitric acid production (around 300–3500 ppm). Indeed, it has been reported that around 10 % of N_2O yearly released into the atmosphere originates from adipic acid production, and therefore much efforts have been made to abate the N_2O deriving from such source. The catalytic N_2O decomposition to N_2 and O_2 is among the most attractive

processes for its abatement, as it does not necessitate any reductant species and renders N_2O abatement possible (at the emission source) at lower temperatures (300-500 °C) than the conventional thermal technology. Not only Cu-ZSM-5 but also several other catalysts demonstrated promising performance in the reaction, including hydrotalcites [4,5], mixed-oxides [6,7], perovskites [8] and other metal-exchanged zeolites [9–12]. When catalyzed by a reducible oxide, the reaction proceeds differently from when catalyzed by a reducible cation- exchanged zeolite: to this respect, Cu-ZSM-5 is one of the most promising candidates for the catalytic N_2O abatement, since it shows relatively higher activity at low temperatures in comparison to other metal-exchanged zeolites, as firstly demonstrated by Li and Armor [13].

However, the most interesting features of Cu-ZSM-5 in this reaction is its ability to induce an oscillatory behavior of the reaction rate under certain reaction conditions. The earliest investigation on the isothermal oscillation of N_2O decomposition over a Cu-ZSM-5 catalyst dates back to 1994, when Lintz and Turek discovered an irregular oscillation of N_2O, NO and O_2 concentrations during an isothermal reaction at 450 °C [14]. A following study by Ciambelli *et al.* demonstrated the effect of both catalyst pre-treatment and reaction temperature on the oscillation pattern and the resulting N_2O conversion [15]. They found that the reducing pre-treatment, during which most of the copper species were reduced to Cu^+, resulted in a shorter transient period and a slightly higher N_2O conversion than the oxidizing pre-treatment. It was also discovered that the oscillation frequency increased with temperature, though too high temperatures (*i.e.* above 400 °C) could quench, or even eliminate, the oscillation. In a separate study, the effect of residence time on the oscillatory behavior and N_2O conversion was also discussed [9]. Specifically, it was reported that a lower residence time helped improving the regularity of the oscillation, finally leading to a higher N_2O conversion.

The oscillatory behavior of N_2O decomposition over Cu-ZSM-5 catalyst was initially associated to periodic changes of copper oxidation states, which exploit the duality of N_2O as both oxidant and reductant species [15]. Based on the premise that both Cu^+ and Cu^{2+} species may coexist in the catalyst, the reaction mechanism proposed by Ciambelli *et al.* is expressed by the following steps (eq. 1-4) [9]:

$$N_2O + 2Cu^+ \rightarrow [Cu\text{-}O\text{-}Cu]^{2+} + N_2 \quad (1)$$

$$N_2O + [Cu\text{-}O\text{-}Cu]^{2+} \rightarrow N_2 + O_2 + 2Cu^+ \quad (2)$$

$$[Cu\text{-}O\text{-}Cu]^{2+} \leftrightarrow O_{ads} + 2Cu^+ \quad (3)$$

$$2O_{ads} \leftrightarrow O_2 \quad (4)$$

Step 1 concerns the adsorption of N_2O on two vicinal Cu^+ sites, which further leads to the formation of mono(μ-oxo)dicopper species, $[Cu - O - Cu]^{2+}$, and, simultaneously, to the reduction to N_2. Step 2 describes the reduction of $[Cu - O - Cu]^{2+}$ species by N_2O back to Cu^+ as well as the decomposition of N_2O to N_2 and O_2. Step 3 and 4 concern the possibility of spontaneous desorption of extra-lattice oxygen (ELO) from $[Cu - O - Cu]^{2+}$ species as dioxygen molecule.

Different rates of those elementary steps were supposed to cause the oscillation: step 1 is the fastest one, due to the presence of active Cu^+ sites, whereas both step 3 and 4 are rate-limiting. Through an operando UV-vis spectroscopy study, Groothaert *et al.* proposed a similar reaction mechanism, where, instead, the step 2 was split into two elementary steps (eq. 5 and 6), involving bis(μ-oxo)dicopper species (eq. 5) as another reaction intermediate [16]:

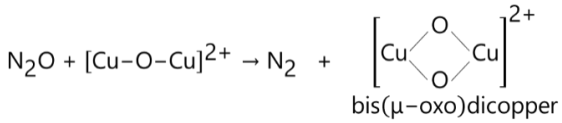

(5)

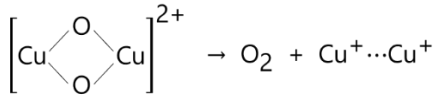

(6)

Being the step 6 rate-limiting, the release of O_2 was supposed to be governed by the reduction of bis(μ-oxo)dicopper species by N_2O back to $[Cu - O - Cu]^{2+}$(eq. 7) and not necessarily to proceed through $Cu^+\cdots Cu^+$ pairs, as in step 6.

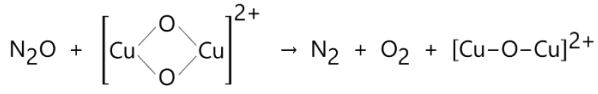

(7)

With the proposed mechanisms, the authors claimed that the reaction and its oscillatory behavior do depend on the oxidation state of copper, which in turn depends of the catalyst preparation technique.

The synthesis of Cu-ZSM-5 by ion-exchange, especially with copper cations in excess with the respect to zeolite sites (namely an "over-exchanged" metal-zeolite), has been adopted in many studies, as it is believed to promote the formation of $[Cu - O - Cu]^{2+}$ species, which actively take part in the reaction [9,17,18]. Less attention, instead, has been paid to other synthesis techniques, such as impregnation and sublimation, which may give rise to different oxidation and dispersion states of copper. An XPS/XAES study by Shpiro *et al.* demonstrated that in over-exchanged Cu-ZSM-5, copper occurred in small clusters or as isolated Cu^+/Cu^{2+} ions (depending on the reaction atmosphere), whilst in impregnated Cu-ZSM-5 copper occurred in large aggregates at the zeolite external surface [19]. Spoto *et al.* proposed a solid-state ion-exchange (SSIE, or sublimation route) synthesis of Cu-ZSM-5 by exchanging the zeolite Brønsted

acid sites with sublimated Cu^+ ions [20,21]: SSIE resulted in isolated Cu^+ sites, easily accessible to probes like carbon monoxide and nitric oxide. Actually, the nature of Cu species in the Cu-ZSM-5 has been widely characterized, but no sure conclusion can be drawn yet, and also in relation to the occurrence of oscillation in the decomposition of N_2O, no sure attribution of responsible Cu species still exists.

In the present work, we explored three different syntheses of Cu-ZSM-5 catalysts, namely wet impregnation, ion-exchange, and SSIE, using the same H-ZSM-5 parent zeolite (Si/Al = 25), trying to obtain catalyst with variable copper loading and observe their effect on the conversion and the isothermal oscillatory behavior of N_2O decomposition. Moreover, a further Cu-ZSM-5 sample was also prepared over a very low Al-containing zeolite (Si/Al = 500) with the purpose to enlighten the effects of not-exchanged copper species. In order to support the results of catalytic activity tests, the catalysts were characterized by means of CO adsorption at room temperature, as followed by IR spectroscopy, and H_2-TPR (Temperature Programmed Reduction).

2. Experimental

2.1. Catalyst synthesis

The H-ZSM-5 support (Si/Al ratio = 25/1) was prepared by calcination of NH_4-ZSM-5 commercial powders (Alfa Aesar) at 550 °C for 5 h in air, while a second sample of H-ZSM-5 characterized by a very low Al content was already available in a commercial H-form (Zeolyst, Si/Al = 500/1). A series of samples were prepared: two Cu-ZSM-5 catalysts with different copper loading were prepared by ion exchange (referred to as CZ-EX-A and CZ-EX-B) and by wet impregnation (CZ-IM-A and CZ-IM-B). A fifth sample was prepared by SSIE and will be referred to as CZ-SU. These five samples were prepared over the parent H-ZSM-5 zeolite characterized by the Si/Al ratio equal to 25. Finally, a further sample were prepared via impregnation over the H-ZSM-5 zeolite characterized by a much higher Si/Al ratio, equal to 500 (CZ-IM-500).

In a typical wet impregnation, 1 g H-ZSM-5 powder was added to 50 mL of 10 mM (sample CZ-IM-A) or 20 mM (sample CZ-IM-B and CZ-IM-500) aqueous solution of $Cu(CH_3COO)_2{\cdot}H_2O$ and the mixture was kept under vigorous stirring at 80 °C, till complete water evaporation. The impregnated zeolite was directly dried overnight at 60 °C and finally treated in a two-step calcination, as detailed below.

In a typical ion exchanged, 50 mL of 10 mM (sample CZ-EX-A) or 20 mM (sample CZ-EX-B) aqueous solution of $Cu(CH_3COO)_2{\cdot}H_2O$ were used to exchange 1g of H-ZSM-5. The mixture was kept under vigorous stirring at 50 °C for 2 h. The ion exchanged zeolite was recovered by centrifugation and repeatedly washed with bidistilled water and ethanol before drying overnight at 60 °C.

The sample CZ-SU was prepared as follows: before sublimation, 0.033 g CuCl and 0.5 g H-ZSM-5 were separately treated under vacuum (10^{-3} mbar) at 100 °C for 2 h and at 400 °C for 3 h, respectively. Then, they were mixed and heated under vacuum in a double-bulb glass cell at 300 °C for 20 min. A final outgassing treatment at 500 °C was carried out in order to remove excess CuCl.

The six catalysts were finally calcined under a reductive environment (333 ml min^{-1} of He at 550 °C for 2 h) and subsequently under a mild oxidative environment (333 ml min^{-1} of 1%-vol O_2 in He gas at 550 °C for 2 h).

2.2. Catalytic activity testing

Before catalytic tests, the catalyst powders were pressed and sieved at the average size of 250 μm. 100 mg catalyst was used in most of the tests. A typical flow-reactor setup with a fixed-bed U-tube Quartz reactor, a K-type thermocouple, a PID-controlled vertical furnace was used in the catalytic activity testing. A non-dispersive infrared (NDIR) analyzer was connected to the reactor exit. Prior to the test, the catalyst was pre-reduced under 200 ml min^{-1} of He at 550 °C for 2 h. The tests were mostly carried out by flowing a 200 ml min^{-1} (W/F ratio = 0.03 cm^3 s, where W = catalyst weight and F = feed gas volumetric flow rate) of 1000 ppm of N_2O in He through the reactor while the reactor temperature was kept isothermal at 400 °C. The reaction under such conditions was kept running for about six hours to better observe the reaction oscillation. A separate set of tests with the same flow conditions was performed by lowering and raising the reaction temperature periodically in the 350 - 450 °C range in order to observe the effect of temperature on the oscillatory behavior. Finally, a set of isothermal tests with different flow conditions was performed by varying the W/F ratio between 0.015 and 0.06 g cm^3 s in order to observe the effect of residence time on the reaction oscillation.

2.3. Catalyst characterization

The catalysts specific surface area (SSA) and total pore volume were measured by N_2 physisorption at -196 °C on powders pre-outgassed at 250 °C for 2 h (Tristar II 3020 Micromeritics). SSA was calculated according to the BET (Brunauer-Emmett-Teller) method, the corresponding values being reported in Table 1, along with other relevant data.

The samples copper loading (wt%) was measured on each sample by energy dispersive X-ray (EDX) analysis (AZTec, Oxford Instruments) on three different areas of about 0.1 mm^2: the average values (wt%) are reported in Table 1.

For IR measurements, the powders were pressed as thin self-supporting wafers (*ca.* 8 mg cm^{-2}) and were outgassed at 500°C for 2 h in a homemade quartz cell equipped with (IR transparent) KBr windows. The IR spectra were recorded at 2 cm^{-1} resolution on a BRUKER EQUINOX-66 spectrometer equipped with a mercury cadmium telluride (MCT) cryodetector. IR spectra were recorded by dosing at room temperature (r.t.) increasing amounts of CO (1-3000 Pa equilibrium pressure range) on the outgassed samples. In order to better allow comparison, the IR spectra in both Figure 6 and 7 were normalized with respect to the integrated absorption of framework overtone bands (2090 – 1550 cm^{-1}), though wafers with very similar area and weight were used. The difference spectra in Figure 7 were obtained by subtracting the IR spectrum of the naked wafer (before CO adsorption): after CO adsorption, an evacuation step at r.t. was performed each time, in order to check the reversibility of the interaction.

The catalysts reducibility was analyzed by H_2-TPR (Temperature Programmed Reduction) on a TPD/R/O instrument (TPDRO 1100, Thermo Scientific). Prior to the analysis, a reductive pre-treatment (40 ml min^{-1} of He at 550 °C) was applied to about 50 mg as-calcined catalyst for 1 h. The TPR analysis was carried out by feeding 20 ml min^{-1} of 5%-v H_2 in Ar to the sample holder and under a gradual heating from r.t. to 800 °C at a rate of 10 °C min^{-1}.

3. Results and discussion

3.1. Textural properties of the catalysts

XRD patterns of the prepared Cu-ZSM-5 samples did not show appreciable differences with respect to the parent zeolite, except with samples CZ-IM-B and CZ-IM-500 (Figure S1 Supporting Information), where two sharp peaks were detected at 2θ = 35.5 and 38.7°, likely due to the formation of bulky CuO at the external surface of the zeolite particles, as confirmed by FESEM analysis (Figure S1).

As far as the metal content is concerned, the Cu wt.% values measured by EDX are reported in Table 1. In principle, the neutralization of two zeolite negative charges by a single divalent Cu^{2+} cation is only possible if the former are sufficiently close, as it may occur in low Si/Al ratio zeolites [22]. On the other hand, monovalent $(Cu^{2+}\text{-}OH)^{+}$ species were found to compensate one zeolite negative charge in ion-exchanged Cu-ZSM-5 samples prepared using copper(II) precursors [23,24]. Thus, only copper loadings larger than 3.7 wt% (corresponding to a Cu/Al ratio of 1 for a H-ZSM-5 with Si/Al = 25) may be actually indicative of excessively-exchanged samples. In contrast, we found that with all samples the Si(OH)Al Brønsted sites were not entirely exchanged (*vide infra*), even with Cu/Al > 1.

The impregnated samples (CZ-IM-A and CZ-IM-B) showed markedly different copper loading, close to the nominal value, whereas just a smaller difference was observed with the ion-exchanged samples (CZ-EX-A

and CZ-EX-B). Actually, the pH of the exchange solution and the copper precursor (acetate *vs* nitrate, for instance) are probably the most determinant factors affecting the eventual copper loading in ion-exchanged samples, as reported in the literature [25]. Residual Cl (0.6 wt.%) was evidenced by EDX measurements in CZ-SU, suggesting the presence of some unreacted CuCl precursor (and/or its derivatives produced during calcination). The presence of Cu- and Cl-containing particles at the external zeolite surface was confirmed by FESEM/EDX analysis (Figure S2). As far as the SSA of the samples is concerned, the values in Table 1 show that the S_{BET} of the Cu-ZSM-5 samples is generally lower than that of the parent H-ZSM-5 (412 m^2 g^{-1}). Both S_{BET} and total pore volume decrease at increasing copper loading. Actually, the copper richest sample (CZ-IM-B, 6.5 wt%) exhibits the lowest values of both S_{BET} (250 m^2 g^{-1}) and pore volume, thus suggesting the presence of CuO aggregates also within the zeolite channels.

3.2. Catalytic activity testing

Figure 1A shows the evolution of N_2O outlet concentration during the isothermal reaction at 400 °C, over the five catalysts prepared on the ZSM-5 sample characterized by the Si/Al ratio equal to 25 (the W/F ratio was maintained at 0.03 g cm^{-3} s in each test).

All the catalysts exhibit a certain activity in the decomposition of N_2O, though quite variable among the different samples. Such a property seems to be basically correlated to the catalyst copper content, rather than to the preparation procedure. For instance, the CZ-EX-A sample is able to convert only about 10% of the fed N_2O, probably because it contains the lowest amount of copper (2.4 wt.%). Conversely, CZ-IM-B can convert about 75% of the fed N_2O, even if the reaction occurs with an oscillation, and indeed it possesses a much higher Cu loading (6.5 wt%). However, with some of the catalysts, the outlet N_2O concentration does not reach a stable and constant value during the time on stream, but exhibits an oscillating pattern, in agreement with previous works [9,14,15]. In particular, the impregnated samples (CZ-IM-A and CZ-IM-B) demonstrate a very pronounced and regular oscillatory behavior, while only the copper richest exchanged zeolite sample (CZ-EX-B) demonstrates a similar pattern. Finally, no oscillations were observed over the CZ-SU sample, notwithstanding its significant N_2O decomposition activity. The CZ-SU sample, indeed, seems to have different copper species, in agreement with the fact that it was prepared by using a Cu^+ precursor (CuCl), whereas both the impregnated and the ion-exchanged samples were prepared by using a Cu^{2+} precursor ($Cu(CH_3COO)_2 \cdot H_2O$). The oscillation induced by CZ-IM-B started quite promptly after the reagent flowed through the catalytic bed, while the reaction over CZ-IM-A

started to oscillate after a delay (or "ignition time") of almost one hour, as occurred in previous works [9,15,18]. Such a delay is also observed with CZ-EX-B, yet it seems shorter than that of CZ-IM-A.

CZ-IM-B provides the highest average N_2O conversion, whereas CZ-IM-A and CZ-EX-B have comparable activity (and Cu content, Table 1). In the decomposition test carried out over CZ-SU, despite the slightly higher Cu content, N_2O conversion reaches about 50%, i.e. it is very similar to the average performances of both CZ-IM-A and CZ-EX-B.

Fig.1B reports the magnification of the oscillation in the time range from 175 to 245 min for the three oscillating catalysts: comparison of the behavior of CZ-IM-A and CZ-IM-B shows that the oscillation frequency seems to increase with the copper content. While the former sample induces a 3.7 mHz oscillation with a regular amplitude (*ca.* 180 ppm), the latter produces a more rapid oscillation with an average frequency of 4.5 mHz and variable amplitudes. The oscillation induced by CZ-EX-B has a remarkable regularity, in that no decay of amplitude is observed even after an overnight test. However, the oscillation occurs at a lower frequency (1.4 mHz) and the maxima of the oscillation seem to last longer than the minima.

3.2.1. Effect of temperature

Figure 2 reports the results of isothermal tests with a step change of temperature carried out over the samples that exhibited the oscillation, namely CZ-IM-A, CZ-IM-B and CZ-EX-B; the temperature step progression was as follows: 350 °C – 375 °C – 400 °C – 375 °C – 400 °C – 350 °C. The lowest temperature range was selected to better observe the sensitivity of the oscillation to the temperature change. It can be observed that the oscillation induced by these three catalysts generally occurs at higher temperatures; the higher the temperature, the higher the oscillation frequency. The topmost plot in Fig.2A shows the test progression over CZ-IM-A. An oscillation with low frequency (at about 1.39 mHz) and low amplitude is observed at 375 °C while at a higher temperature the oscillation becomes very regular and has a much higher frequency (about 3.13 mHz). At 350 °C, the oscillation is not observed, probably due to a too short isotherm duration. The N_2O conversion in this range of temperature spans from 15% to 50%, the highest conversion being achieved at 400 °C.

The middle plot in Figure 2A summarizes the test progression over CZ-IM-B: the conversion span is clearly much higher than with the other two catalysts in the series (about 50% at 375 °C and 80% at 400 °C). Likewise, the oscillation pattern induced by the catalyst varies with temperature: lower-frequency oscillation is observed at the lower temperature (1.85 mHz at 375 °C) and high-frequency oscillation is

observed at higher temperature (4.17 mHz at 400 °C). On the second repetition, the oscillation frequency at 375 °C slightly decreases to about 1.67 mHz while that at 400 °C decreases to 3.70 mHz.

The bottommost plot in Fig.2A reports the test progression over CZ-EX-B: the sample exhibits a unique behavior, in that it induces a very low frequency oscillation. At the lowest temperature, the oscillation seems to be nonexistent, and the conversion is very low (almost 5%). During the second isotherm, where the temperature was increased by 25 °C, the reaction hardly oscillated except right towards the end of the isotherm, where a "valley" of N_2O concentration appears, presumably marking the beginning of the oscillation. This temperature step was eventually repeated right after the completion of the first isotherm at 400 °C and was carried out almost twice as long to allow the oscillation to occur. In this step, a regular oscillation occurred very slowly at a frequency of 0.49 mHz (almost equal to 2 oscillations per hour). At 400 °C, the oscillation appears more frequent at an average frequency of 1.28 mHz and the temperature switch does not seem to affect the oscillation at the same temperature in the second repetition. Because of the long oscillation induction time, we repeated the isotherm at 350 °C in the last step for few more hours. After about 3 h of a flat, non-oscillating reaction, the concentration of N_2O oscillated very slowly at a frequency of about 0.18 mHz, which is almost equal to 2 oscillations in 3 h (see the inset). As previously seen in Fig.1, CZ-EX-B is the only sample in the series whose oscillation takes a unique form; the duration of the maxima is incomparably longer than that of the minima.

Similar tests were also conducted for CZ-EX-A and CZ-SU, the two samples that did not induce an oscillatory behavior during the reaction at the previously investigated temperature (400 °C). The conversion range was smaller for CZ-EX-A, but larger for CZ-SU (up to 80% at the highest temperature). We have performed the tests with a longer duration per isothermal step, yet we have never observed any oscillations during the reactions.

3.2.2. Further insight into the oscillations' phenomenon

Figure 3 analyses in more detail what happens during the oscillations of the rate of N_2O decomposition in the entire gas phase. As it will be done in the following graphs, Figure 1 and 2 show the pattern of the concentration of the unconverted N_2O at the reactor outlet as detected by a continuous gas analyzer. This is done for the sake of simplicity, but the adopted system allows analyzing the outlet concentration profiles of O_2, NO and NO_2 too.

Looking at the plots reported in Figure 3 related to a kinetic test carried out over CZ-IM-A chosen as representative sample, the oscillation of the outlet concentration of N_2O are accompanied by the

oscillations of the produced O_2, and by the oscillating by-production of NO and NO_2, as well. The average production of molecular oxygen is basically in agreement with the average conversion of nitrous oxide, although the shape of the two signals appear not specular and in some way, different. Different considerations can be made on NO_x formation ($NO+NO_2$) which are not expected from the stoichiometry of pure N_2O decomposition. In fact, Turek [26] already observed the production a certain amount of NO in the oscillating decomposition of N_2O, while Fanson et al. [27] provided spectroscopic evidence that surface nitrate species are present under oscillatory conditions. Thus, Fanson et al. proposed a slow build-up of surface nitrates during oscillating cycle, followed by the rapid nitrate decomposition responsible of an increase in the rate of N_2O decomposition.

The present results are in agreement with those previous findings. We found the by-production of both NO and NO_2, *i.e.* two secondary products of N_2O conversion (actually, products of the oxidation of N_2O and not of its decomposition). They are always present in a simultaneous way and at a fixed NO/NO_2 ratio (probably at its thermodynamically limited value), because the interconversion of NO into NO_2 is strongly activated by Cu-ZSM-5 [28], and can be roughly estimated with a selectivity of around 3-4% with respect to the amount of converted N_2O. Such a NO_x by-production occurs in form of spikes or peaks appearances, rather than proper oscillations. Such spikes appear to be simultaneous for both NO and NO_2, but also for O_2. Actually the oscillations of O_2 appear to much less irregular than those of the unconverted nitrous oxide. Such a peak production of O_2, NO and NO_2 always occurs at the beginning of the period of maximum activity of the catalyst towards the decomposition of N_2O, since the concentration of the unconverted nitrous oxide is at its minimum in the cycle and the oxygen production is reaching its maximum in the oscillation' period. Moreover, the mass balance is consistent with the over-emission of NO_3-like species, whose accumulation and subsequent decomposition was proposed by Fanson et al. [27]. Such a behavior is a general trend for all the N_2O decomposition tests, where the oscillations have been observed.

A further test of N_2O decomposition was carried out also over the CZ-IM-500 sample (Figure 4), with the purpose of enlightening the effects of not-exchanged copper species. Surprisingly, despite the presence of very few exchangeable sites due to the low Al content (Si/Al = 500), the catalyst does possess a very weak, though measurable, activity in the decomposition of N_2O. We can evaluate around 4-5% N_2O conversion, as also confirmed by the production of the corresponding and stoichiometric amount of O_2. However, even if somewhat surprising, such results indirectly confirm that the ionically exchanged Cu species are responsible for the activity in the N_2O decomposition, since the level of measured activity is

very far from what expected on the mere copper content (6.2 %wt.). The comparison with the results reported in Figure 1 is blatantly revealing the difference.

Even more unexpectedly, we observed a sort of dynamic and periodic behavior of both N_2O and O_2 outlet concentration too, as well as of the by produced NO and NO_2. We may describe it as the appearance of "oscillations", even if a careful look reveals that the phenomenon would be better described observing the appearance of periodic peaks of products production and peaks of reactant consumption over stable values of concentration. It is clear that the peak of O_2 production is associated to the peak of N_2O over-consumption, and it is simultaneous to the peak production of NO and NO_2 (with same level of selectivity observed over the CZ samples characterized by a much lower Si/Al). However, such a phenomenon shows a period of the same order of magnitude of that observed for the oscillations over the Cu-ZSM-5 catalysts prepared from parent zeolite with Si/Al = 25.

3.2.3. Effect of residence time

Figure 5 finally summarizes the results from the isothermal tests with various W/F ratios. Only the oscillation-inducing catalysts, namely CZ-IM-A, CZ-IM-B and CZ-EX-B, were tested. Previous experiments were conducted with constant W/F ratio (0.03 g cm^{-3} s), whereas in this series of experiments, the temperature was kept constant at 400 °C while the W/F ratio was halved (0.015 g cm^{-3} s) and doubled (0.06 g cm^{-3} s). The plots in Fig.3A show the complete transient profile of N_2O outlet concentration within the first hours of the tests, during which the eventual ignition of the unsteady-state phenomenon occurs, while in Fig.3B the respective magnified profiles are reported with the purpose of better analyzing the oscillating phenomenon and accurately characterizing its features. Generally, it appears evident that, over all the three catalysts, the oscillatory behavior is significantly affected by the contact time. Doubling the W/F ratio to 0.06 g cm^{-3} s obviously leads to an increment of N_2O conversion. The effect of the W/F ratio on the oscillations seems to be not negligible, as a general trend of frequency enhancement with increasing W/F is observed over all the samples. However, in the case of the impregnated samples at the longest residence time explored, the oscillations seem to decay. Such an effect is not observed with CZ-EX-B, over which the phenomenon is still observed, even after a much longer induction time (two hours of transitory period). Finally, the features of the oscillation induced by CZ-EX-B at such W/F ratio differ from those at lower W/F ratio; indeed, besides showing lower amplitude, the oscillation maxima have a shorter duration than the minima, as if the superimposition of two different phenomena was taking place.

The results of the catalytic activity tests showed a stronger correlation of the N_2O conversion to the catalyst copper content rather than to the adopted preparation technique. On the other hand, the

oscillatory behavior seems to depend on the type of copper precursor: indeed, the use of copper (I) precursor leads to a non-oscillating system. The effect of temperature on both reaction conversion and oscillatory behavior is clear: the higher the temperature, the higher the conversion, and the higher the oscillation frequency. The effect of residence time is clearly observed on the conversion, yet it cannot be neglected on the oscillatory behavior: whilst a higher residence time always leads to higher N_2O conversion, in certain cases, it leads to an oscillation decay.

3.3. Catalysts characterization

In order to shed light on the species responsible for the different catalysts behavior, we focused on the characterization of four representative samples prepared by different procedures, *i.e.* CZ-IM-B, CZ-EX-A, CZ-EX-B, and CZ-SU. The first one showed the highest N_2O conversion and an oscillatory behavior; the second one showed limited conversion and no oscillatory behavior; the last two showed a comparable N_2O conversion, but only CZ-EX-B showed the oscillatory behavior.

3.3.1. IR spectroscopy study of CO adsorption at r.t.

3.3.1.1. Consumption of Brønsted acidic sites after exchange procedures

The O–H stretching region of the IR spectra of the parent H-ZSM-5 zeolite and the selected Cu-ZSM-5 samples pre-treated under vacuum at 500°C is reported in Figure 6. The parent H-ZSM-5 (curve 1) shows a sharp peak at 3745 cm^{-1}, a broad and weak absorption centered at 3660 cm^{-1} and an intense band at 3610 cm^{-1}. The three bands are respectively assigned to the O–H stretching vibrations of *(i)* defective Si-OH groups (silanols, mostly located at the zeolite external surface), *(ii)* extra-framework Al-OH groups, stemming from dealumination, and *(iii)* bridged Si-(OH)-Al groups (Brønsted acidic sites) [21,29].

With the Cu-ZSM-5 samples (curves 2-5), the band of Brønsted sites is only partially consumed, independently of the synthesis procedure. The ratio between the integrated absorbance of the 3610 cm^{-1} band of the parent H-ZSM-5 and of the same band in the exchanged samples was used to calculate the exchange percentages ($\%_{EX}$) reported in Table 1. It has to be noticed that with respect to the nomenclature introduced by Iwamoto *et al.* [30] (*i.e.* Cu/Al = 0.5 for 100% exchange), the values in the Table 1 simply refer to the percentage of exchanged Brønsted sites (independently of the copper oxidation state). Ion-exchanged samples showed the lowest $\%_{EX}$, *i.e.* 47 (CZ-EX-A) and 50 $\%_{EX}$ (CZ-EX-B). Notably, the double concentration of the exchange solution used for CZ-IE-B yielded an increase in the copper content (2.4 vs 3.8 wt%), but only a slightly higher $\%_{EX}$. In principle, if zeolite negative charges

were balanced by monovalent $(Cu^{2+}\text{-}OH)^{+}$ species, a copper content not exceeding 1.79 and 1.90 wt% should be found for 47 and 50 $\%_{EX}$ (for Si/Al = 25). Based on this analysis, the percentages of copper ions in exchange position (*% Cu_Z* in Table 1) is ca. 75 (for CZ-EX-A) and 49 % total copper (for CZ-EX-B). The obtained *% Cu_Z* must be taken as maximum limit values, since they were calculated by assuming that each copper ion exchanges one Brønsted site (lower values would be obtained by assuming that a single Cu^{2+} ion can exchange two Brønsted sites). The Cu species not directly exchanging zeolite acidic protons are clearly more abundant for sample CZ-EX-B. These may include: *i)* CuO particles formed by decomposition (during calcination) of precipitated $Cu(OH)_2$ phase; *ii)* Cu species exchanging external Si-OH groups; *iii)* oligomeric Cu_xO_y structures with extra-lattice oxygen (ELO) formed within zeolite channels. The mild pH (5.6 - 5.8) and concentration (20 and 40 mM) of the exchange solutions should in principle limit the precipitation of $Cu(OH)_2$. Actually, both IR spectroscopy of adsorbed CO and H_2-TPR (*vide infra*) of CZ-EX-B showed the possible presence of limited amount of CuO particles, which were not detected by XRD and FESEM. In contrast, with CZ-EX-B only, the integrated absorbance of the Si-OH band at 3745 cm^{-1} was almost halved, suggesting that also some of the external Si-OH groups were exchanged, as previously observed with copper/silica systems [31]. Finally, the formation of structures with ELO resulting from the hydrolysis of hexaaquacopper(II) complex $[Cu(H_2O)_6]^{2+}$ and its polycondensation reactions is likely to occur at the adopted exchange temperature and concentration [2][32][33], and is supported by the pore volume values. Notably, divalent structures with ELO like those represented in eq. (3) and (5) (*i.e.* oxo- and bis(μ-oxo)-dicopper species) cannot contribute to the copper excess if bridged on two zeolitic sites. Rather, polyoxocations with a number of Cu ions ≥ 2 and with one (or two) positive charges should exchange one (or two) Brønsted sites. The fate of such species upon calcination and reducing treatment is uncertain. One possibility is the formation of easily reducible Cu_Z^{2+} ions bridged with Cu_xO_y oligomers via oxo- (or bis(μ-oxo)) bridges. On the other hand, Ismagilov et al. [34][35] observed the formation of 1D chain-like structures (*e.g.* --- O^{2-}---Cu^{2+}---O^{2-}--- Cu^{2+}--- O^{2-}---) stabilized inside the channels of dehydrated Cu-ZSM-5 samples prepared by ion-exchange with aqueous copper acetate solutions at 60 and 80°C. The chain structures were found to be easily reduced and re-oxidized, being even capable of self-reduction, and stabilizing states of copper ions with mixed valence Cu^{2+}/Cu^{+}, *i.e.* showing those features that are believed to be indispensable for the oscillating behavior.

With respect to ion-exchanged samples, higher $\%_{EX}$ are obtained with CZ-SU (71 %) and CZ-IM-B (68%), corresponding to a *% Cu_Z* of 60 and 39 %, respectively. With CZ-SU, the Cu species not in exchange position mostly consist of unreacted CuCl precursor and its derivatives produced during calcination, whereas the Si-OH groups were not exchanged. As expected, sample CZ-IM-B showed the largest copper

loading but the lower *% Cu_Z*. Indeed, the impregnation method, besides yielding exchanged ionic species, results in the formation of significant amount of *i)* CuO particles (both intra- and extra-porous) formed by Cu acetate decomposition during calcination, and *ii)* Cu_xO_y structures with ELO formed within zeolite channels. Finally, also with CZ-IM-B, the Si-OH groups were not exchanged, although the copper precursor solution was the same as for CZ-EX-B: this could be due to the solvent evaporation during impregnation, implying a pH increase that likely disfavors Si-OH deprotonation/exchange [31].

3.3.1.2. CO adsorption at r.t.

CO adsorption at r.t. as followed by IR spectroscopy is widely used in the characterization of Cu-ZSM-5 [21,25,29,36–39]: Figure 7 reports difference spectra obtained after dosing CO (1 – 5000 Pa) on the selected Cu-ZSM-5 samples. The main features are the IR bands due to the formation of mono- (2157 cm^{-1}) and di-carbonyl (2177 and 2150 cm^{-1}) complexes on exchanged Cu^+ ions (Cu_Z^+) [21,29]. Besides those, a shoulder at *ca.* 2135 cm^{-1} is observed with CZ-SU, CZ-IM-B and, to a lesser extent, with CZ-EX-B. Moreover, mono-carbonyl complexes forming on Cu_Z^+ are not reversible upon outgassing at r.t..

At low coverage, a strong absorption ascribed to $Cu_Z^+(CO)$ complexes is observed at 2157 cm^{-1}: such species are progressively consumed with increasing CO equilibrium pressure, and simultaneously two bands, due to symmetric (2177 cm^{-1}) and asymmetric (2150 cm^{-1}) stretching modes of $Cu_Z^+(CO)_2$ complexes, grow in intensity. The isosbestic point at *ca.* 2153 cm^{-1} clearly indicates that the di-carbonyl species form at the expense of the former. Interestingly, the isosbestic point is well defined with CZ-SU and CZ-EX-A (which does not shows an oscillating behavior), but not with CZ-EX-B and CZ-IM-B. Such a difference suggests the possible heterogeneity of Cu_Z^+ sites in the latter samples. Actually, several works reported the existence of at least two kinds of Cu^+ sites in Cu-ZSM-5 [29,36–38]. In particular, it was shown that CO molecules are strongly adsorbed on Cu^+ sites coordinated by two lattice oxygen atoms (the corresponding IR band absorbing at 2159 cm^{-1}), whereas are weakly adsorbed on Cu^+ sites coordinated by three lattice oxygen atoms (the corresponding IR band absorbing at 2151 cm^{-1}) [36,37]. The presence of Cu_xO_y structures with ELO close to a Cu^+ site in exchange position may actually be the reason of the observed heterogeneity. Such hypothesis seems to be confirmed by comparing the integrated absorbance of the symmetric and asymmetric IR stretching modes of the di-carbonyl complexes on the four samples. Normalized difference IR spectra obtained at the same CO equilibrium pressure (*i.e.* 1,2 kPa) were curve-fitted by using five components with Voigt profiles, the results of which are shown in Figure S3 (Supporting Information). Notably, the ratio between the integrated absorbance of the bands at 2177 cm^{-1} and 2150 cm^{-1} is much smaller for CZ-IM-B and CZ-EX-B (0.25 and 0.22,

472 respectively) with respect to CZ-SU and CZ-EX-A (0.40 and 0.35, respectively). Such observation suggests
473 that there may be an additional IR component that contributes to the intensity of the band 2150 cm^{-1} in
474 CZ-IM-B and CZ-EX-B, in agreement with the broader FWHM of such band (9.4, 8.1, 7.5 and 6.1 cm^{-1} for
475 CZ-IM-B, CZ-EX-B, CZ-SU and CZ-EX-A respectively). According to ref [36] and [37], mono-carbonyl
476 complexes on weaker Cu^+ sites may form at a higher CO equilibrium pressure (*i.e.* where stronger sites
477 already form di-carbonyl complexes), thus giving rise to an IR band overlapping to that of di-carbonyl
478 complexes at 2150 cm^{-1}. This interpretation would be in agreement with the different sharpness of the
479 isosbestic point at 2153 cm^{-1}. The different ability to coordinate one or two CO molecules may depend on
480 the different coordination sphere of Cu_Z^+, which could be affected by the vicinity of Cu_xO_y structures with
481 ELO. Interestingly, the two samples characterized by such type of heterogeneity are those showing the
482 oscillating behavior in the catalytic tests.
483 Besides IR bands due to carbonyl species forming on Cu^+ sites in exchange position (Cu_Z^+), the
484 assignment of the shoulder at 2135 cm^{-1} that starts to grow at a low coverage in IR spectra concerning
485 with CZ-SU is not straightforward. Spoto *et al.* observed a similar shoulder (though located at 2142 cm^{-1})
486 on a sample prepared by SSIE and assigned it to mono-carbonyl complexes formed on CuCl aggregates
487 that were either trapped in the zeolite channels or located at the external surface of the zeolite particles.
488 Notably, Cu^+–CO complexes absorbing at 2132-2137 cm^{-1} have also been observed to form on both
489 supported Cu_2O and CuO [25,39,40]. Indeed, heat treatment under vacuum is known to yield reduction of
490 some Cu^{2+} to Cu^+ at the CuO particles surface [41,42]. Actually, the presence of both CuO and CuCl in CZ-
491 SU were evidenced by H_2-TPR (*vide infra*) and EDX measurements (Table 1), thus supporting both the
492 assignments. On the other hand, H_2-TPR measurements evidenced the presence of CuO on CZ-IM-B and,
493 to a lesser extent, on CZ-EX-B. Thus, the shoulder observed at 2135 cm^{-1} in the IR spectra of CZ-IM-B may
494 is assigned to Cu^+–CO complexes forming onto the partially reduced surface of some CuO particles. This
495 assignment is supported by CO adsorption onto CZ-IM-500 sample (Figure S4), for which both XRD and
496 TPR showed the presence of CuO particles. Indeed, the IR spectra taken at increasing CO coverage onto
497 CZ-IM-500 showed, as a main feature, a band at 2132 cm^{-1} (shifting to 2127 cm^{-1} with coverage) assigned
498 to Cu^+–CO complexes forming onto the partially reduced surface of CuO. Weak bands due to mono- and
499 di-carbonyls forming on exchanged Cu^+ sites are also observed, but their intensity is definitely lower than
500 that observed with CZ-IM-B, according to the lower Al content.
501 Finally, the weak band at 2108 cm^{-1} (observed with all the Cu-ZSM-5 samples and stable after evacuation
502 at r.t.) could be due to either CO molecules adsorbed through the O end [43] or the adsorption of CO
503 molecules on reduced copper species (*i.e.* Cu^0-CO) present, however, in a minor amount [44].

3.3.2. H_2-TPR analysis

Figure 8 shows the H_2-TPR spectra of the pre-reduced catalysts. Usually, the reduction of copper species in zeolites occurs in two ranges of temperatures: namely, below 300 °C, where reduction of Cu^{2+} to Cu^{+} and/or to Cu^{0} occurs, and above 300 °C, where reduction of Cu^{+} to Cu^{0} occurs [44–46].

In most of the samples, the reduction ends at relatively low temperatures, *i.e.* below 400-450°C, as expected for samples loaded with excess copper. Only with CZ-EX-A, the second reduction peak is observed at 510°C. Actually, Bulánek *et al.* showed that the last peak position in Cu-ZSM-5 H_2-TPR spectra is shifted to a higher temperature at decreasing copper contents [45].

The H_2-to-Cu molar ratios (H/Cu) of the investigated samples (*i.e.* the ratio between the total consumption of H_2 and the total amount of Cu measured by EDX) are between 0.5 (corresponding to 100% Cu(I)) and 1.0 (corresponding to 100% Cu(II)), as reported in Table 1. CZ-IM-500 sample shows an H/Cu ratio close to unity, in agreement with the presence of mainly CuO particles, the surface of which displays only some Cu^{2+} ions able to undergo self-reduction (not quantifiable by TPR but evidenced by FTIR). In contrast, a lower ratio is observed with CZ-IM-B (*i.e.* 0.90, corresponding to 80% Cu(II)), indicating the presence of a fraction of Cu (II) species able to undergo self-reduction. These latter likely include both exchanged Cu_Z^{2+} species and the above mentioned structures with ELO. On the other hand, the samples prepared by ion-exchange with Cu acetate showed higher H/Cu ratio, *i.e.* 0.85 (corresponding to 72% Cu(II) in CZ-EX-A) and 0.81 (corresponding to 62% Cu(II) in CZ-EX-B). Between these two samples, CZ-EX-B has a larger amount of Cu (II) species able to undergo self-reduction, although showing similar $\%_{EX}$. This observations seems to confirm that the use of more concentrated exchange solution favors the formation oligomeric Cu_xO_y structure with ELO rather increasing the amount of isolated Cu_Z^{2+} ion in exchange position. Finally, the lowest H/Cu ratio was obtained with sample CZ-SU, *i.e.* 0.65, corresponding to 30% Cu(II). Given the mild calcination conditions, the most obvious reason for this value would be the oxidation state of the copper precursor.

A quantitative analysis of the TPR spectra aimed at determining the H_2 consumption due to the different copper species is not straightforward. Indeed, the overlapping of the temperature ranges at which the different species are reduced hinders a precise quantitative correlation between the area of the reduction peaks and the abundance of the different copper species. Indeed, at least four different copper species may occur in the samples: (1) exchanged copper(II) ions (Cu_Z^{2+}); (2) exchanged copper(I) ions (Cu_Z^{+}); (3) segregated CuO particles and (4) Cu_xO_y structures with ELO. Moreover, the segregated CuO species may differ in size and location (inside or outside the pores). Supported CuO is generally reduced to Cu^{0} in a

single autocatalytic step, the greater its dispersion, the lower its reduction temperature [47,48]. This reduction behavior is observed with sample CZ-IM-500, showing a single asymmetric reduction peak with maximum at 280°C and shoulder at 247°C. According to IR and XRD results, the very low Al content of the impregnated sample results in the formation of mainly supported CuO particles and negligible amounts of Cu_Z species, the latter being responsible of the very weak H_2 consumption at ca. 380°C. The asymmetry of the main peak may be due to CuO particles of different size (*e.g.* large particles on the outer surface and clusters within channels).

According to the literature [45,49,50], the Cu_Z^{2+} species are expected to be reduced in two steps: $Cu^{2+} + ½ H_2 \rightarrow Cu^+$ (that generally occurs at T < 250°C), and $Cu^+ + ½ H_2 \rightarrow Cu^0$ (that generally occurs at T > 300°C). Therefore, if all Cu_Z were present as copper(II) (*i.e.* in the absence of self-reduction phenomena), two equivalent peaks would be expected at low and high temperature, respectively, while the occurrence of self-reduction during He pre-treatment would result in a decrease of the first H_2 consumption. This is what we observed with CZ-EX-A, *i.e.* the sample with the lowest copper content (2.4 wt.%), but the highest % Cu_z (75% total copper). Two distinct reduction peaks at 240 (ca. 154 μmol g_{cat}^{-1}) and 507°C (ca. 166 μmol g_{cat}^{-1}) are observed. The lower H_2 consumption of the first peak is consistent with the occurrence of self-reduction during the He pre-treatment. The first peak is markedly asymmetric towards high temperatures and, besides the reduction of Cu_Z^{2+} to Cu_Z^{+}, it may include the reduction of the Cu^{2+} of structures with ELO. On the other hand, the H_2 consumption of the second peak fairly matches the value calculated from % Cu_Z (ca. 140 μmol g_{cat}^{-1}).

With respect to CZ-EX-A, the spectrum of CZ-EX-B shows three main different features: (1) the high temperature peak is more intense and shifted towards lower temperatures (*i.e.* 335 °C), strongly overlapping those at low-temperature; (2) a weak sharp central peak appears at 275°C; (3) the low temperature peak (244 °C) shows higher H_2 consumption.

The increase in H_2 consumption occurring during the high temperature reduction step cannot be justified only by the slight increase in the $\%_{EX}$ (47 and 50%, with CZ-EX-A and CZ-EX-B, respectively). Indeed, the reduction of the Cu^{2+} species exchanging external Si-OH groups, the presence of which was evidenced by the consumption of the band at 3745 cm^{-1} (*vide supra*), could also occur in this temperature range. The high peak temperature indicates a strong metal-support interaction, rendering the species less reducible. Bond *et al.* reported that (less reducible) dispersed Cu^{2+} species in a CuO/SiO_2 system were reduced in the temperature range of 300 – 350 °C [51]. Chang *et al.* has also confirmed the presence of such Cu^{2+} species (chemically interacting with a silica support) and their reducibility in a similar temperature range [52].

As far as the central peak (at 275 °C) is concerned, the sharp shape and the temperature range correspond to an autocatalytic reduction process involving limited amounts of CuO cluster within zeolite channels, not detected by XRD and FESEM, but evidenced by IR spectroscopy (weak shoulder at 2135 cm^{-1}). Finally, the increase in H_2 consumption during the low temperature peak is mainly due to the larger amount of Cu_xO_y structures with ELO. We cannot exclude that part of such structures is reduced in a two-step process [34], thus also contributing to the high temperature H_2 consumption .

The spectrum of CZ-IM-B is characterized by an intense and asymmetric peak, with a maximum at 258°C and two shoulders at ca. 230 and 280°C, and a broad peak at 330°C. H_2 consumption at T < 300°C is due to superimposition of (at least) three peaks. Actually, in this temperature range, the reduction of Cu_Z^{2+}, Cu_xO_y species with ELO within zeolite channels, and CuO particles occur. According to the assignments done for CZ-IM-500 and CZ-EX-B, and to the trend observed in pore volumes, the components at 258 and 282 °C are assigned to extra-porous and intra-porous CuO particles, whereas the low temperature shoulder (not present with CZ-EX-500) corresponds to the reduction of Cu_Z^{2+} and Cu_xO_y species with ELO.

Notwithstanding the relatively high $\%_{EX}$ measured with this sample (*i.e.* 68%), the peak due to the reduction of Cu_Z^{+} (330 °C) appears less intense than that of the other samples. This feature is consistent with the presence of CuO clusters in the close proximity of some Cu_Z^{2+} ions, which could be therefore reduced directly to Cu(0) in a single reduction step.

Finally, the TPR spectrum of CZ-SU shows a profile and total H_2 consumption similar to those of CZ-EX-B, but lower H/Cu ratio. Furthermore, the sharp central peak is significantly shifted toward higher temperatures (316°C), being unlikely due to CuO. We assigned this peak to residual CuCl aggregates probably trapped in the zeolite channels: actually, reduction of CuCl takes place at higher temperatures with respect to CuO [53,54]. Furthermore, the measured H/Cu ratio indicates the presence of only 30% Cu(II). Given that a copper(I) precursor and mild calcination conditions were adopted, the majority of exchanged copper after He pre-treatment is likely present as Cu_z^{+}. It follows that most of Cu^{2+} is located in segregated Cu-containing species, which could also imply the occurrence of some oxidation products of unreacted CuCl, *e.g.* CuO and $Cu_2(OH)_3Cl$, the latter species being likely responsible for the reduction peaks at ca. 240°C

4. Conclusions

The study of the possible effects of the preparation procedure of Cu-ZSM-5 samples on the spontaneous oscillations occurring during the catalytic decomposition of N_2O provided relevant evidence of the presence of various type of copper species in the Cu containing ZSM-5 catalysts. The unsteady-state

oscillatory phenomenon did not occur with all the prepared catalysts; in fact, we demonstrated that a series of peculiar features should be exhibited by the samples for the oscillations to occur. First, a minimum amount of copper is required to obtain a certain activity in the reaction as well as to observe the establishment of a periodic oscillating pattern of the unconverted N_2O concentration at the reactor outlet or (which, by the way, is the same) of the N_2O conversion and of the decomposition rate.

Interestingly, a complete exchange level (*i.e.* complete consumption of Brønsted acid sites) was not observed even with the samples with high copper content (Cu/Al>1). However, in addition to the amount of exchanged sites, also the nature of copper "excess" have a crucial role in both activity and oscillating behavior. The comparison between CZ-EX-A (scarce activity, and no oscillations) and CZ-EX-B (good activity, and oscillations) is emblematic, as both sample showed similar exchange level. The same conclusions are obtained by comparing the samples with higher Cu_Z content, *i.e.* CZ-SU (good activity, but no oscillations) and CZ-IM-B (superior activity, and pronounced oscillations).

The oscillatory phenomenon could be associated with the occurrence of oligomeric Cu_xO_y species with extra-lattice oxygen (*e.g* chains or clusters) able to undergo reduction/oxidation cycles. Such species may form by ion-exchange with polyoxocations resulting from the hydrolysis of hexaaquacopper(II) complex $[Cu(H_2O)_6]^{2+}$ and its polycondensation reactions, and are more abundant in excessively-exchanged (*i.e.*Cu/Al > 1) samples prepared by either impregnation or ion-exchange. In contrast, they lack in CZ-SU, *i.e.* the sample prepared by sublimation of copper(I) chloride, which, correspondingly, did not give rise to oscillations. In CZ-SU, the exchanged copper species seem to be almost exclusively isolated Cu^+ ions that, even after a mild calcination, cannot be oxidized to Cu^{2+} ions, and most of all are not present in aggregated forms. In this way, the kind of Cu species present in the CZ-SU sample, even if quite active in the decomposition of N_2O, prevents the reaction to occur over both active sites, and hence in an unstable equilibrium between the two oxidation states.

References

[1] H.-Y. Chen, Cu/Zeolite SCR Catalysts for Automotive Diesel NOx Emission Control, in: I. Nova, E. Tronconi (Eds.), Urea-SCR Technol. DeNOx After Treat. Diesel Exhausts, Springer, New York, NY, 2014: pp. 123–147. doi:https://doi.org/10.1007/978-1-4899-8071-7_5.

[2] S. Yashnik, Z. Ismagilov, Cu-substituted ZSM-5 catalyst: Controlling of DeNOx reactivity via ion-exchange mode with copper-ammonia solution, Appl. Catal. B Environ. 170–171 (2015) 241–254. doi:10.1016/j.apcatb.2015.01.021.

[3] Y. Li, J.N. Armor, Catalytic reduction of nitrogen oxide with methane in the presence of excess oxygen, Appl. Catal. B Environ. 1 (1992) L31–L40. doi:10.1016/0926-3373(92)80050-A.

[4] J.N. Armor, T.A. Braymer, T.S. Farris, Y. Li, F.P. Petrocelli, E.L. Weist, S. Kannan, C.S. Swamy, Calcined hydrotalcites for the catalytic decomposition of N2O in simulated process streams, Appl. Catal. B Environ. 7 (1996) 397–406. doi:10.1016/0926-3373(95)00048-8.

[5] S. Kannan, C.S. Swamy, Catalytic decomposition of nitrous oxide over calcined cobalt aluminum hydrotalcites, Catal. Today. 53 (1999) 725–737. doi:10.1016/S0920-5861(99)00159-5.

[6] F.J. Perez-Alonso, I. Melián-Cabrera, M. López Granados, F. Kapteijn, J.L.G. Fierro, Synergy of $Fe_xCe_{1-x}O_2$ mixed oxides for N_2O decomposition, J. Catal. 239 (2006) 340–346. doi:10.1016/J.JCAT.2006.02.008.

[7] F. Kapteijn, J. Rodriguez-Mirasol, J.A. Moulijn, Heterogeneous catalytic decomposition of nitrous oxide, Appl. Catal. B Environ. 9 (1996) 25–64. doi:10.1016/0926-3373(96)90072-7.

[8] N. Russo, D. Mescia, D. Fino, G. Saracco, V. Specchia, N_2O Decomposition over Perovskite Catalysts, Ind. Eng. Chem. Res. 46 (2007) 4226-4231 doi:10.1021/IE0612008.

[9] P. Ciambelli, A. Di Benedetto, E. Garufi, R. Pirone, G. Russo, Spontaneous Isothermal Oscillations in N_2O Decomposition over a Cu–ZSM5 Catalyst, J. Catal. 175 (1998) 161–169. doi:10.1006/JCAT.1998.1986.

[10] B.I. Palella, M. Cadoni, A. Frache, H.O. Pastore, R. Pirone, G. Russo, S. Coluccia, L. Marchese, On the hydrothermal stability of CuAPSO-34 microporous catalysts for N_2O decomposition: a comparison with CuZSM-5, J. Catal. 217 (2003) 100–106. doi:10.1016/S0021-9517(03)00033-2.

[11] J.A.. Pieterse, S. Booneveld, R. van den Brink, Evaluation of Fe-zeolite catalysts prepared by different methods for the decomposition of N2O, Appl. Catal. B Environ. 51 (2004) 215–228. doi:10.1016/J.APCATB.2004.02.013.

[12] F. Kapteijn, G. Marbán, J. Rodriguez-Mirasol, J.A. Moulijn, Kinetic Analysis of the Decomposition of Nitrous Oxide over ZSM-5 Catalysts, J. Catal. 167 (1997) 256–265. doi:10.1006/JCAT.1997.1581.

[13] Y. Li, J.N. Armor, Catalytic decomposition of nitrous oxide on metal exchanged zeolites, Appl. Catal. B Environ. 1 (1992) L21–L29. doi:10.1016/0926-3373(92)80019-V.

[14] H.-G. Lintz, T. Turek, Isothermal oscillations in the catalytic decomposition of nitrous oxide over Cu-ZSM-5, Catal. Letters. 30 (1995) 313–318. doi:10.1007/BF00813698.

[15] P. Ciambelli, E. Garufi, R. Pirone, G. Russo, F. Santagata, Oscillatory behaviour in nitrous oxide decomposition on over-exchanged Cu-ZSM-5 zeolite, Appl. Catal. B Environ. 8 (1996) 333–341. doi:10.1016/0926-3373(95)00065-8.

[16] M.H. Groothaert, K. Lievens, H. Leeman, B.M. Weckhuysen, R.A. Schoonheydt, An operando optical fiber UV–vis spectroscopic study of the catalytic decomposition of NO and N_2O over Cu-ZSM-5, J. Catal. 220 (2003) 500–512. doi:10.1016/J.JCAT.2003.08.009.

[17] W. Gruenert, N.W. Hayes, R.W. Joyner, E.S. Shpiro, M.R.H. Siddiqui, G.N. Baeva, Structure, Chemistry, and Activity of Cu-ZSM-5 Catalysts for the Selective Reduction of NOx in the Presence of Oxygen, J. Phys. Chem. 98 (1994) 10832–10846. doi:10.1021/j100093a026.

[18] R. Pirone, E. Garufi, P. Ciambelli, G. Moretti, G. Russo, Transient behaviour of Cu-overexchanged

671 ZSM-5 catalyst in NO decomposition, Catal. Letters. 43 (1997) 255–259.
672 doi:10.1023/A:1018967328681.

673 [19] E.S. Shpiro, W. Grünert, R.W. Joyner, G.N. Baeva, Nature, distribution and reactivity of copper
674 species in over-exchanged Cu-ZSM-5 catalysts: an XPS/XAES study, Catal. Letters. 24 (1994) 159–
675 169. doi:10.1007/BF00807386.

676 [20] G. Spoto, S. Bordiga, D. Scarano, A. Zecchina, Well defined $Cu^{I}(NO)$, $Cu^{I}(NO)_2$ and $Cu^{II}(NO)X$ (X = O^-
677 and/or NO_2^-) complexes in Cu^{I}-ZSMS prepared by interaction of H-ZSM5 with gaseous CuCl,
678 Catal. Letters. 13 (1992) 39–44. doi:10.1007/BF00770945.

679 [21] G. Spoto, A. Zecchina, S. Bordiga, G. Ricchiardi, G. Martra, G. Leofanti, G. Petrini, Cu(I)-ZSM-5
680 zeolites prepared by reaction of H-ZSM-5 with gaseous CuCl: Spectroscopic characterization and
681 reactivity towards carbon monoxide and nitric oxide, Appl. Catal. B Environ. 3 (1994) 151–172.
682 doi:10.1016/0926-3373(93)E0032-7.

683 [22] M. Shelef, Selective Catalytic Reduction of NOx with N-Free Reductants, Chem. Rev. 95 (1995) 209–
684 225. doi:10.1021/cr00033a008.

685 [23] S.C. Larsen, A. Aylor, A.T. Bell, J.A. Reimer, Electron Paramagnetic Resonance Studies of Copper Ion-
686 Exchanged ZSM-5, J. Phys. Chem. 98 (1994) 11533–11540. doi:10.1021/j100095a039.

687 [24] J. Dedecek, Z. Sobalik, Z. Tvaruazkova, D. Kaucky, B. Wichterlova, Coordination of Cu Ions in High-
688 Silica Zeolite Matrixes. Cu^+ Photoluminescence, IR of NO Adsorbed on Cu^{2+}, and Cu^{2+} ESR Study, J.
689 Phys. Chem. 99 (1995) 16327–16337. doi:10.1021/j100044a020.

690 [25] S.A. Yashnik, Z.R. Ismagilov, Zeolite ZSM-5 containing copper ions: The effect of the copper salt
691 anion and NH_4OH/Cu^{2+} ratio on the state of the copper ions and on the reactivity of the zeolite in
692 DeNOx, Kinet. Catal. 57 (2016) 776–796. doi:10.1134/S0023158416060161.

693 [26] T. Turek, A transient kinetic study of the oscillating N_2O decomposition over Cu-ZSM-5, J. Catal.
694 (1998). doi:10.1006/jcat.1997.1941.

695 [27] P.T. Fanson, M.W. Stradt, W.N. Delgass, Catalysis Letters, Catal. Letters. 77 (2001) 15–19.
696 https://doi.org/10.1023/A:1012726809704.

697 [28] R. Pirone, P. Ciambelli, G. Moretti, G. Russo, Nitric oxide decomposition over Cu-exchanged ZSM-5
698 with high Si/Al ratio, Appl. Catal. B Environ. (1996). doi:10.1016/0926-3373(95)00068-2.

699 [29] C. Lamberti, S. Bordiga, M. Salvalaggio, and G. Spoto, A. Zecchina*, F. Geobaldo, G. Vlaic, M.
700 Bellatreccia, XAFS, IR, and UV−Vis Study of the CuI Environment in CuI-ZSM-5, (1997).
701 doi:10.1021/JP9601577.

702 [30] M. Iwamoto, H. Yahiro, K. Tanda, N. Mizuno, Y. Mine, S. Kagawa, Removal of nitrogen monoxide
703 through a novel catalytic process. 1. Decomposition on excessively copper-ion-exchanged ZSM-5
704 zeolites, J. Phys. Chem. 95 (1991) 3727–3730. doi:10.1021/j100162a053.

705 [31] M.A. Kohler, J.C. Lee, D.L. Trimm, N.W. Cant, M.S. Wainwright, Preparation of Cu/SiO_2 catalysts by
706 the ion-exchange technique, Appl. Catal. 31 (1987) 309–321. doi:10.1016/S0166-9834(00)80699-5.

707 [32] R. N. Sylva, M.R. Davidson, The Hydrolysis of Metal Ions. Part 1. Copper(II), J. Chem. Soc., Dalton
708 Trans. (1979) 232 –235 DOI: 10.1039/DT9790000232

709 [33] D.D. Perrin, The hydrolisis of Copper (II) Ion., J. Chem. Soc. (1960) 3189–3196.

710 doi:10.1039/JR9600003189.

711 [34] Z.R. Ismagilov, S.A. Yashnik, V.F. Anufrienko, T. V. Larina, N.T. Vasenin, N.N. Bulgakov, S. V. Vosel,
712 L.T. Tsykoza, Linear nanoscale clusters of CuO in Cu-ZSM-5 catalysts, Appl. Surf. Sci. 226 (2004) 88–
713 93. doi:10.1016/j.apsusc.2003.11.035.

714 [35] S.A. Yashnik, Z.R. Ismagilov, V.F. Anufrienko, Catalytic properties and electronic structure of copper
715 ions in Cu-ZSM-5, Catal. Today. 110 (2005) 310–322. doi:10.1016/j.cattod.2005.09.029.

716 [36] R. Kumashiro, Y. Kuroda, M. Nagao, New Analysis of Oxidation State and Coordination
717 Environment of Copper Ion-Exchanged in ZSM-5 Zeolite, J. Phys. Chem. B 103 (1998) 89-96
718 doi:10.1021/JP981935T.

719 [37] Y. Kuroda, R. Kumashiro, T. Yoshimoto, M. Nagao, Characterization of active sites on copper ion-
720 exchanged ZSM-5-type zeolite for NO decomposition reaction, Phys. Chem. Chem. Phys. 1 (1999)
721 649–656. doi:10.1039/a809447k.

722 [38] J. Dědeček, B. Wichterlová, Role of Hydrated Cu Ion Complexes and Aluminum Distribution in the
723 Framework on the Cu Ion Siting in ZSM-5, J. Phys. Chem. B. 101 (1997) 10233–10240.
724 doi:10.1021/JP971776Y.

725 [39] K.I. Hadjiivanov, M.M. Kantcheva, D.G. Klissurski, IR study of CO adsorption on Cu-ZSM-5 and
726 CuO/SiO_2 catalysts: σ and π components of the Cu^+—CO bond, J. Chem. Soc., Faraday Trans. 92
727 (1996) 4595–4600. doi:10.1039/FT9969204595.

728 [40] D. Scarano, S. Bordiga, C. Lamberti, G. Spoto, G. Ricchiardi, A. Zecchina, C. Otero Areán, FTIR study
729 of the interaction of CO with pure and silica-supported copper(I) oxide, Surf. Sci. 411 (1998) 272–
730 285. doi:10.1016/S0039-6028(98)00331-8.

731 [41] L. Yuan, Q. Yin, Y. Wang, G. Zhou, CuO reduction induced formation of CuO/Cu2O hybrid oxides,
732 Chem. Phys. Lett. 590 (2013) 92–96. doi:10.1016/J.CPLETT.2013.10.040.

733 [42] S. Poulston, P.M. Parlett, P. Stone, M. Bowker, Surface Oxidation and Reduction of CuO and Cu_2O
734 Studied Using XPS and XAES, Surf. Interface Anal. 24 (1996) 811–820. doi:10.1002/(SICI)1096-
735 9918(199611)24:12<811::AID-SIA191>3.0.CO;2-Z.

736 [43] S. Bordiga, E. Escalona Platero, C. Otero Areán, C. Lamberti, A. Zecchina, Low temperature CO
737 adsorption on Na-ZSM-5 zeolites: An FTIR investigation, J. Catal. 137 (1992) 179–185.
738 doi:10.1016/0021-9517(92)90147-A.

739 [44] J. Sárkány, J.L. d'Itri, W.M.H. Sachtler, Redox chemistry in excessively ion-exchanged Cu/Na-ZSM-5,
740 Catal. Letters. 16 (1992) 241–249. doi:10.1007/BF00764336.

741 [45] R. Bulánek, B. Wichterlová, Z. Sobalík, J. Tichý, Reducibility and oxidation activity of Cu ions in
742 zeolites: Effect of Cu ion coordination and zeolite framework composition, Appl. Catal. B Environ.
743 31 (2001) 13–25. doi:10.1016/S0926-3373(00)00268-X.

744 [46] T. Nanba, S. Masukawa, A. Ogata, J. Uchisawa, A. Obuchi, Active sites of Cu-ZSM-5 for the
745 decomposition of acrylonitrile, Appl. Catal. B Environ. 61 (2005) 288–296.
746 doi:10.1016/J.APCATB.2005.05.013.

747 [47] C.-H. Tu, A.-Q. Wang, M.-Y. Zheng, X.-D. Wang, T. Zhang, Factors influencing the catalytic activity
748 of SBA-15-supported copper nanoparticles in CO oxidation, Appl. Catal. A Gen. 297 (2006) 40–47.
749 doi:10.1016/J.APCATA.2005.08.035.

[48] Z. Liu, M.D. Amiridis, Y. Chen, Characterization of CuO Supported on Tetragonal ZrO2 Catalysts for N_2O Decomposition to N_2, (2005). doi:10.1021/JP046368Q.

[49] J.Y. Yan, W.M.H. Sachtler, H.H. Kung, Effect of Cu loading and addition of modifiers on the stability of Cu/ZSM-5 in lean NOx reduction catalysis, Catal. Today. 33 (1997) 279–290. doi:10.1016/S0920-5861(96)00100-9.

[50] S. Tanabe, H. Matsumoto, Activation Process of CuY Zeolite Catalyst Observed by TPR and EXAFS Measurements, Bull. Chem. Soc. Jpn. 63 (1990) 192–198. doi:10.1246/bcsj.63.192.

[51] G.C. Bond, S.N. Namijo, J.S. Wakeman, Thermal analysis of catalyst precursors: Part 2. Influence of support and metal precursor on the reducibility of copper catalysts, J. Mol. Catal. 64 (1991) 305–319. doi:10.1016/0304-5102(91)85140-W.

[52] F.-W. Chang, W.-Y. Kuo, K.-C. Lee, Dehydrogenation of ethanol over copper catalysts on rice husk ash prepared by incipient wetness impregnation, Appl. Catal. A Gen. 246 (2003) 253–264. doi:10.1016/S0926-860X(03)00050-4.

[53] Y. Zhang, I.J. Drake, A.T. Bell, Characterization of Cu-ZSM-5 Prepared by Solid-State Ion Exchange of H-ZSM-5 with CuCl, Chem. Mater. 18 (2006) 2347–2356. doi:10.1021/CM052291M.

[54] M.. Jia, W.. Zhang, T.. Wu, The role of copper species and Brønsted acidity in CuCl/ZSM-5 catalysts during the selective catalytic reduction of NO by propene, J. Mol. Catal. A Chem. 185 (2002) 151–157. doi:10.1016/S1381-1169(01)00523-4.

Table 1. Summary of physicochemical properties of the prepared catalysts

Sample[a]	Cu loading (wt%)[b]	Cu/Al[b]	S_{BET} (m^2 g^{-1})[c]	V_p (cm^3 g^{-1})[d]	$\%_{EX}$[e]	% Cu_Z[g]	H_2-to-Cu ratio[h]	% Cu(II) (atomic %)[i]
CZ-IM-A	3.6	1.19	360	0.21	-	-	-	-
CZ-IM-B	6.5	1.9	250	0.16	68	32	0.90	80
CZ-EX-A	2.4	0.82	388	0.24	47	75	0.85	72
CZ-EX-B	3.8	1.12	370	0.22	50	49	0.81	62
CZ-SU	4.5	1.39	355	0.21	71	60	0.65	30

[a] IM = impregnation; EX = ion exchange; SU = sublimation

[b] Cu weight percentage and Cu/Al atomic as measured by EDX

[c] total specific surface area as measured by N_2 physisorption

[d] total pore volume as measured by N_2 physisorption

[e] percentage of exchange obtained from the intensity ratio between the integrated IR absorbance of the 3610 cm^{-1} band in the parent H-ZSM-5 and of the same band in exchanged samples

[g] $(Cu_Z/Cu_{TOT})*100$ = relative abundance of exchanged Cu species on total copper content, as calculated combining $\%_{EX}$ and Cu loading

[h] hydrogen consumption to loaded copper quantity ratio extracted from H_2-TPR and EDX

[i] relative abundance of copper (II) species calculated from H_2-to-Cu ratio, assuming that the moles of consumed H_2 equal the sum of the Cu^{2+} moles of and half of the Cu^{+} moles

792

793 **Caption to Figures**

794 **Figure 1**. Outlet concentration of N_2O as a function of time during the catalytic activity testing under
795 isothermal condition (A) and magnification of the oscillatory behavior of CZ-IM-A, CZ-EX-B and CZ-IM-B
796 (B). Test condition: N_2O feed concentration = 1000 ppm, T = 400°C, W/F = 0.03 g cm^{-3} s. Color legend:
797 magenta (CZ-IM-A), blue (CZ-IM-B), yellow (CZ-EX-A), green (CZ-EX-B), violet (CZ-SU).

798

799 **Figure 2.** Outlet concentration of N_2O (straight line) and reactor temperature (dashed line) as a function
800 of time (A) during the catalytic activity testing with oscillation-inducing catalysts under various isothermal
801 conditions and magnification of the oscillatory behavior of the three catalysts (B). Test condition: N_2O feed
802 concentration = 1000 ppm, W/F = 0.03 g cm^{-3} s. Color legend: magenta (CZ-IM-A), blue (CZ-IM-B) and
803 green (CZ-EX-B).

804

805 **Figure 3.** Composition of the gas at the reactor outlet during the catalytic activity testing under
806 isothermal condition of the sample CZ-IM-B: outlet concentration of N_2O and O_2 (A) and of NO and NO_2
807 (B) as a function of time. Test condition: N_2O feed concentration = 1000 ppm, T = 400°C, W/F = 0.03 g
808 cm^{-3} s. Color legend: magenta (N_2O), blue (O_2), green (NO), black (NO_2).

809

810 **Figure 4.** Composition of the gas at the reactor outlet during the catalytic activity testing under
811 isothermal condition of the sample CZ-IM-500: outlet concentration of N_2O and O_2 (A) and of NO and
812 NO_2 (B) as a function of time. Test condition: N_2O feed concentration = 1000 ppm, T = 400°C, W/F = 0.03
813 g cm^{-3} s. Color legend: magenta (N_2O), blue (O_2), green (NO), black (NO_2).

814

815 **Figure 5.** Effect of residence time on the behavior of the reaction mediated by oscillation-inducing
816 catalysts under isothermal condition. (A) Outlet N_2O concentration as a function of time and (B)
817 magnification of the oscillatory behavior. Test condition: N_2O feed concentration = 1000 ppm, T = 400 °C.
818 Color legend: magenta (CZ-IM-A), blue (CZ-IM-B) and green (CZ-EX-B).

819

820 **Figure 6.** IR spectra of the OH stretching region of the parent H-ZSM-5 zeolite (curve 1), CZ-IM-A (curve
821 2), CZ-IM-B (curve 3), CZ-EX-B (curve 4) and CZ-SU (curve 5) pre-treated under vacuum at 500°C.

822

Figure 7. IR spectra of CO adsorbed at increasing equilibrium pressure (10 – 3000 Pa) on CZ-EX-B (section a), CZ-IM-B (section b), CZ-EX-A (section c) and CZ-SU (section d) at room temperature. Insets show magnification of the isosbestic point.

Figure 8. H_2-TPR spectra of CZ-IM-500, CZ-IM-B, CZ-SU, CZ-EX-B and CZ-EX-A samples pre-treated in He at 550°C.

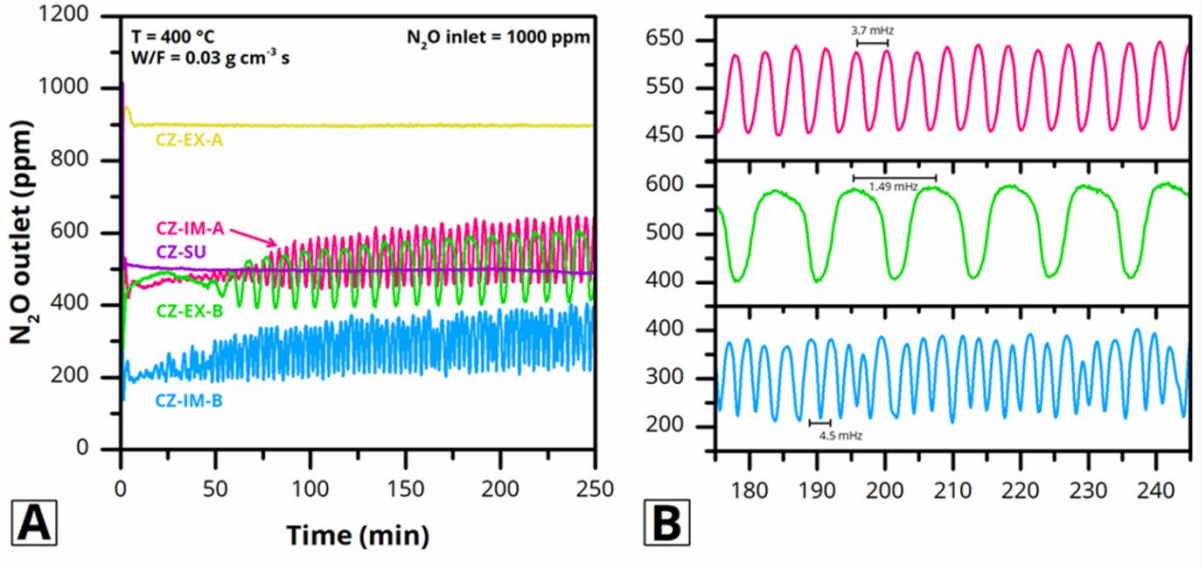

832

833 **Figure 1**

834

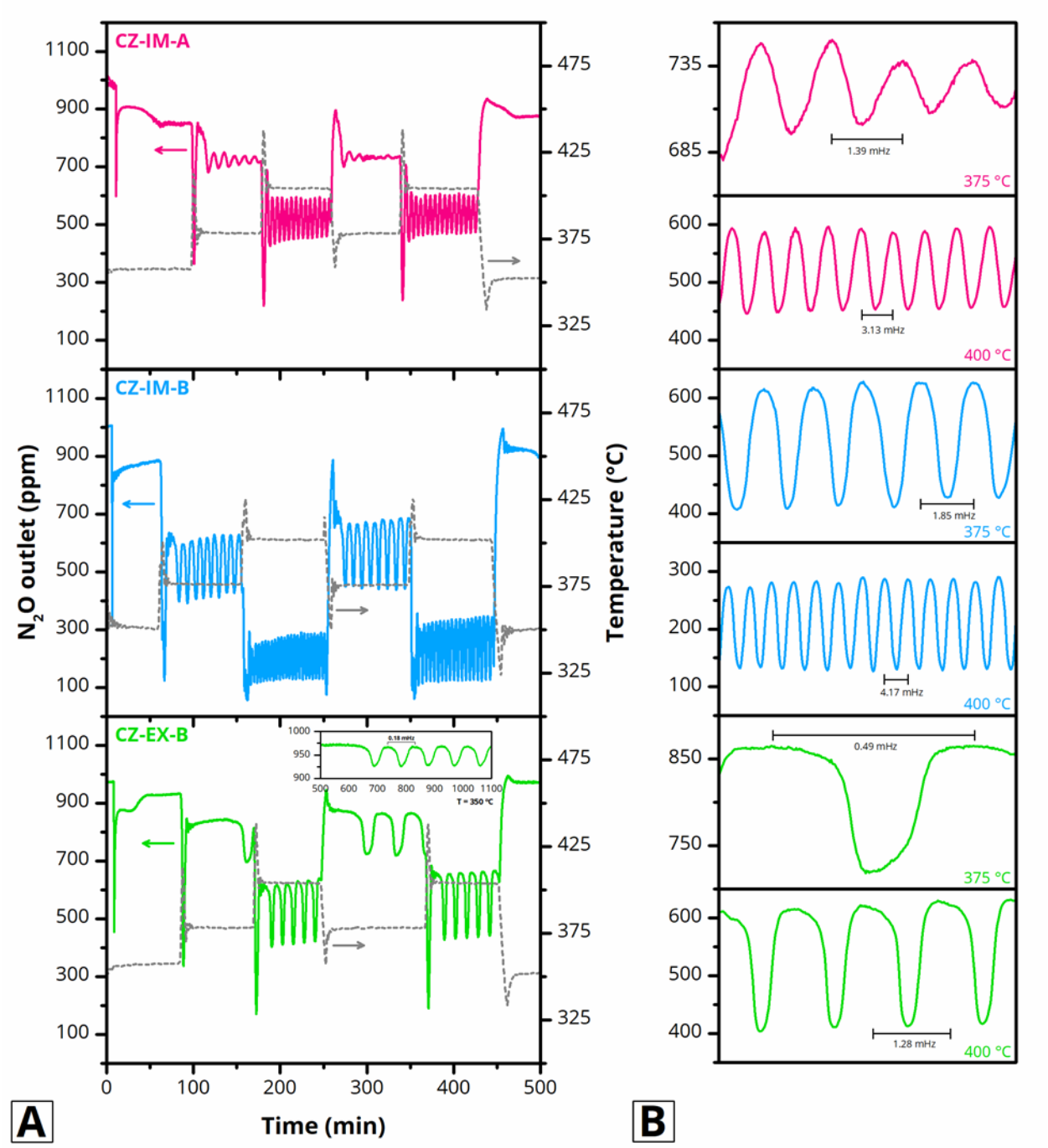
CZ-IM-A
CZ-IM-B
CZ-EX-B
N2O outlet (ppm)
Temperature (°C)
Time (min)
A
B
1.39 mHz
375 °C
3.13 mHz
400 °C
1.85 mHz
375 °C
4.17 mHz
400 °C
0.49 mHz
375 °C
1.28 mHz
400 °C

Figure 2

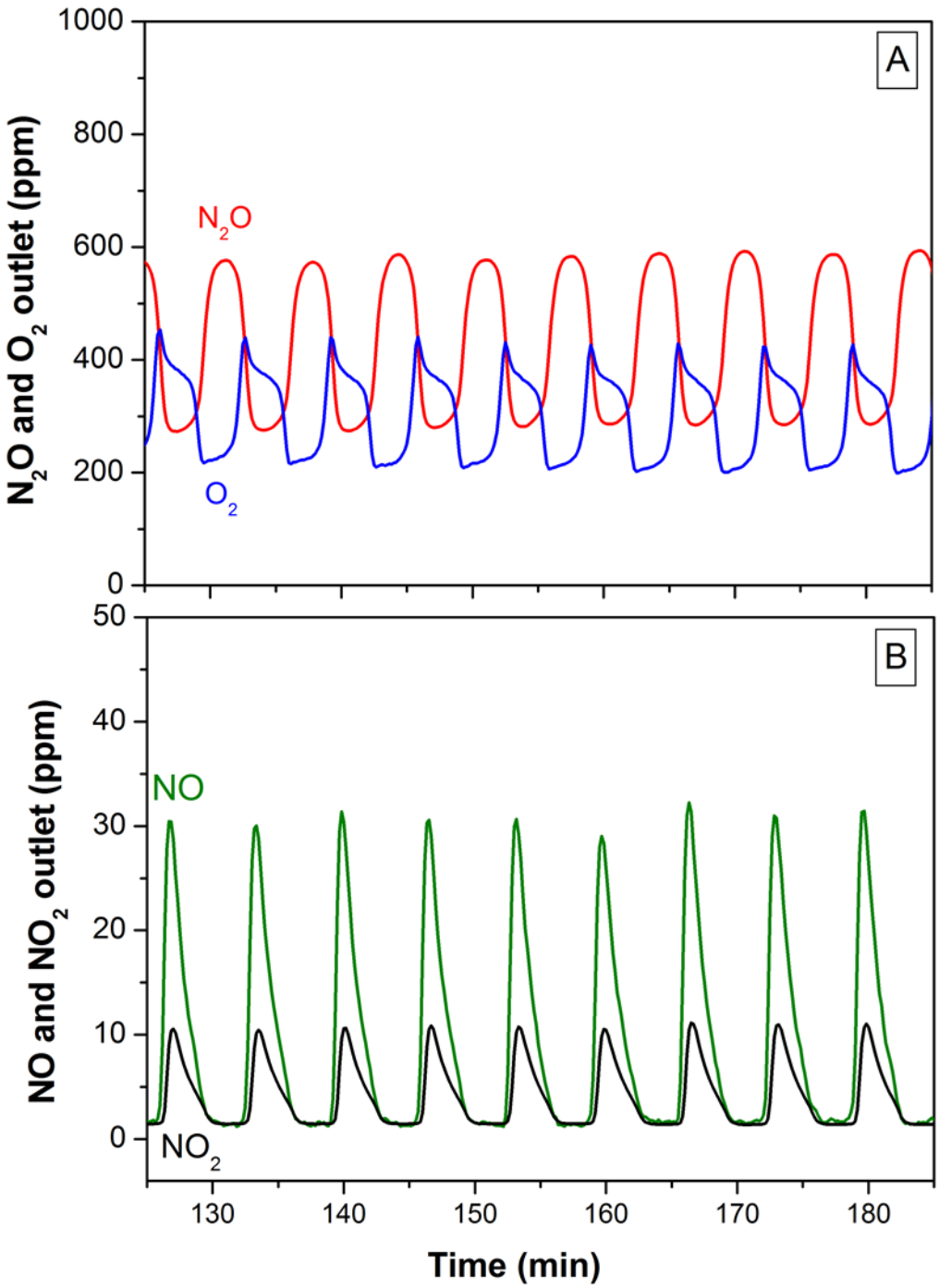

839

840 **Figure 3**

841

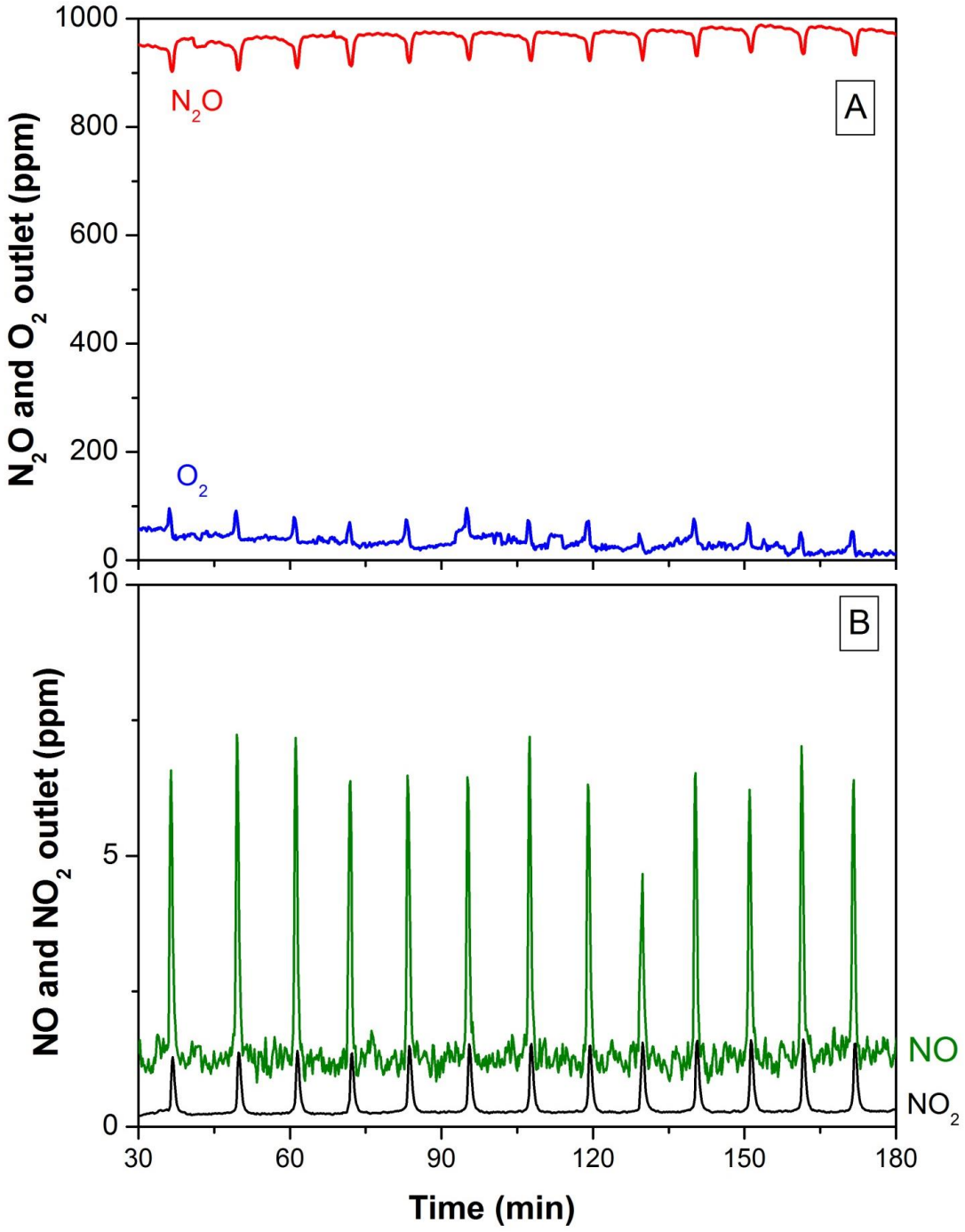

842

843 **Figure 4**

844

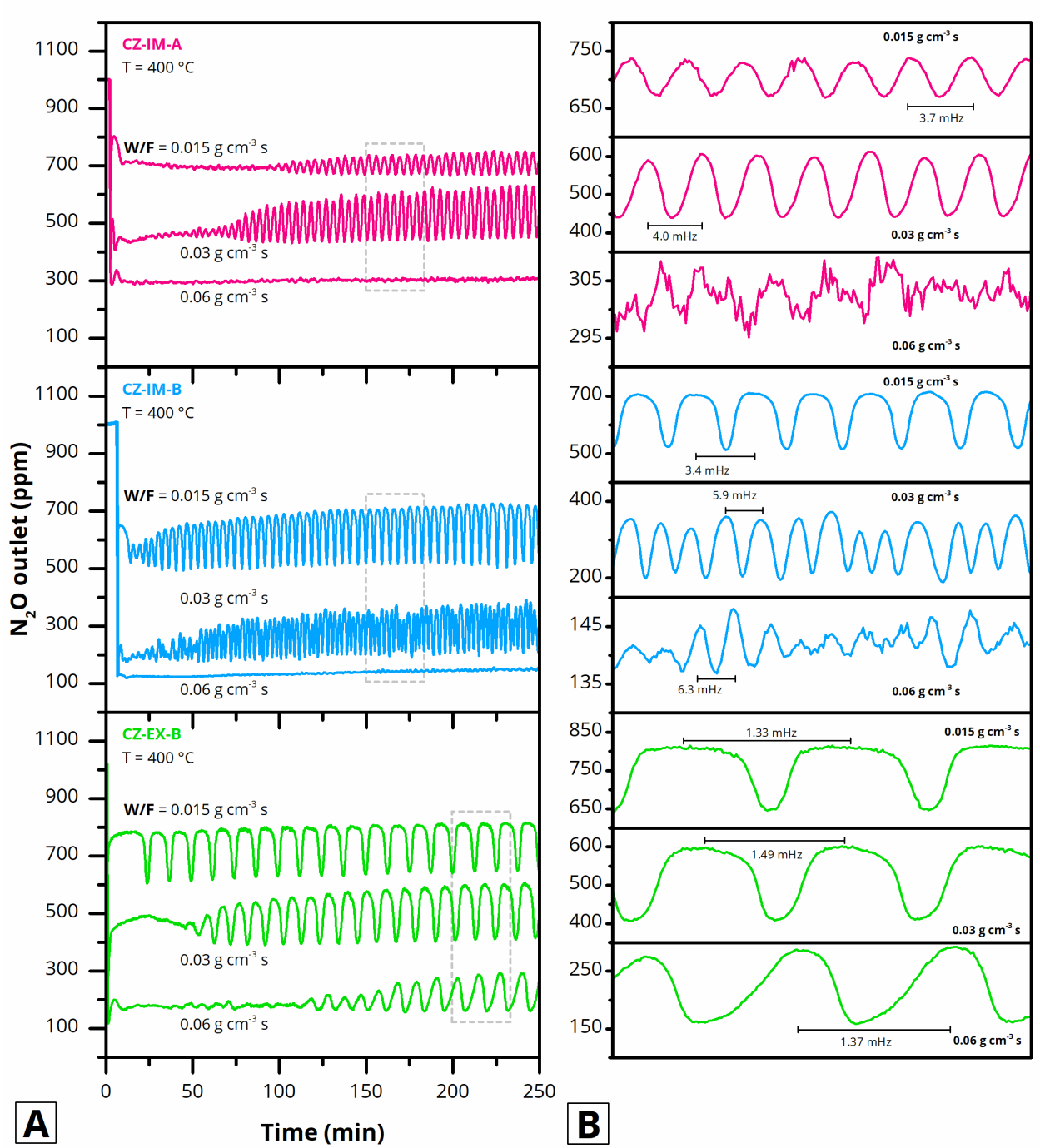
CZ-IM-A
T = 400 °C
W/F = 0.015 g cm-3 s
0.03 g cm-3 s
0.06 g cm-3 s
CZ-IM-B
T = 400 °C
W/F = 0.015 g cm-3 s
0.03 g cm-3 s
0.06 g cm-3 s
CZ-EX-B
T = 400 °C
W/F = 0.015 g cm-3 s
0.03 g cm-3 s
0.06 g cm-3 s
N2O outlet (ppm)
Time (min)
A
B
0.015 g cm-3 s
3.7 mHz
4.0 mHz
0.03 g cm-3 s
0.06 g cm-3 s
3.4 mHz
5.9 mHz
6.3 mHz
1.33 mHz
1.49 mHz
1.37 mHz

Figure 5

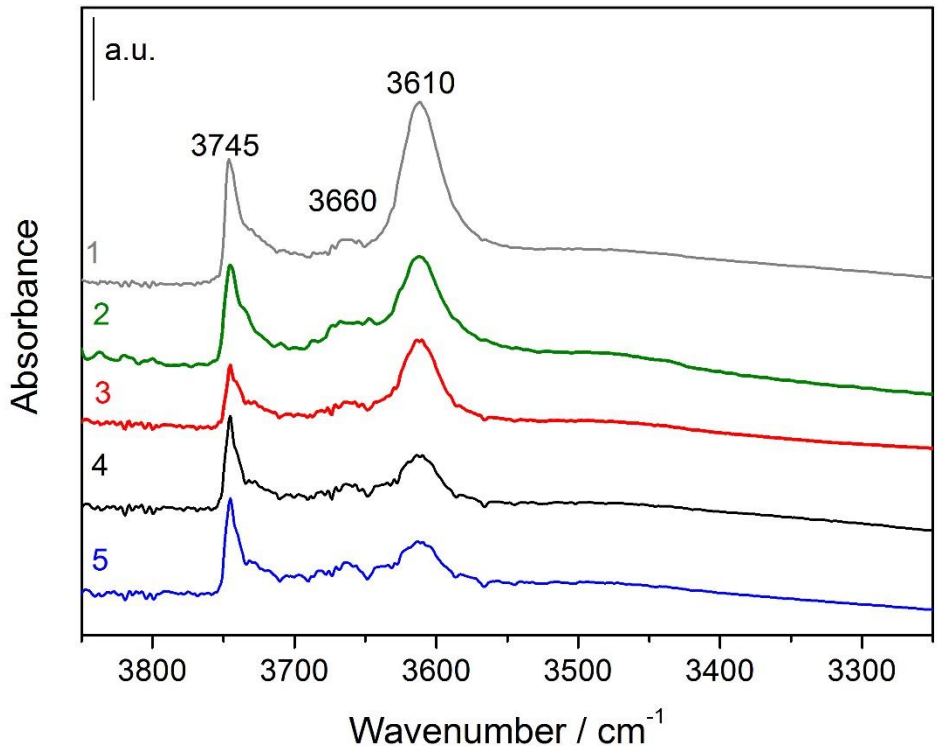

849

850 **Figure 6**

851

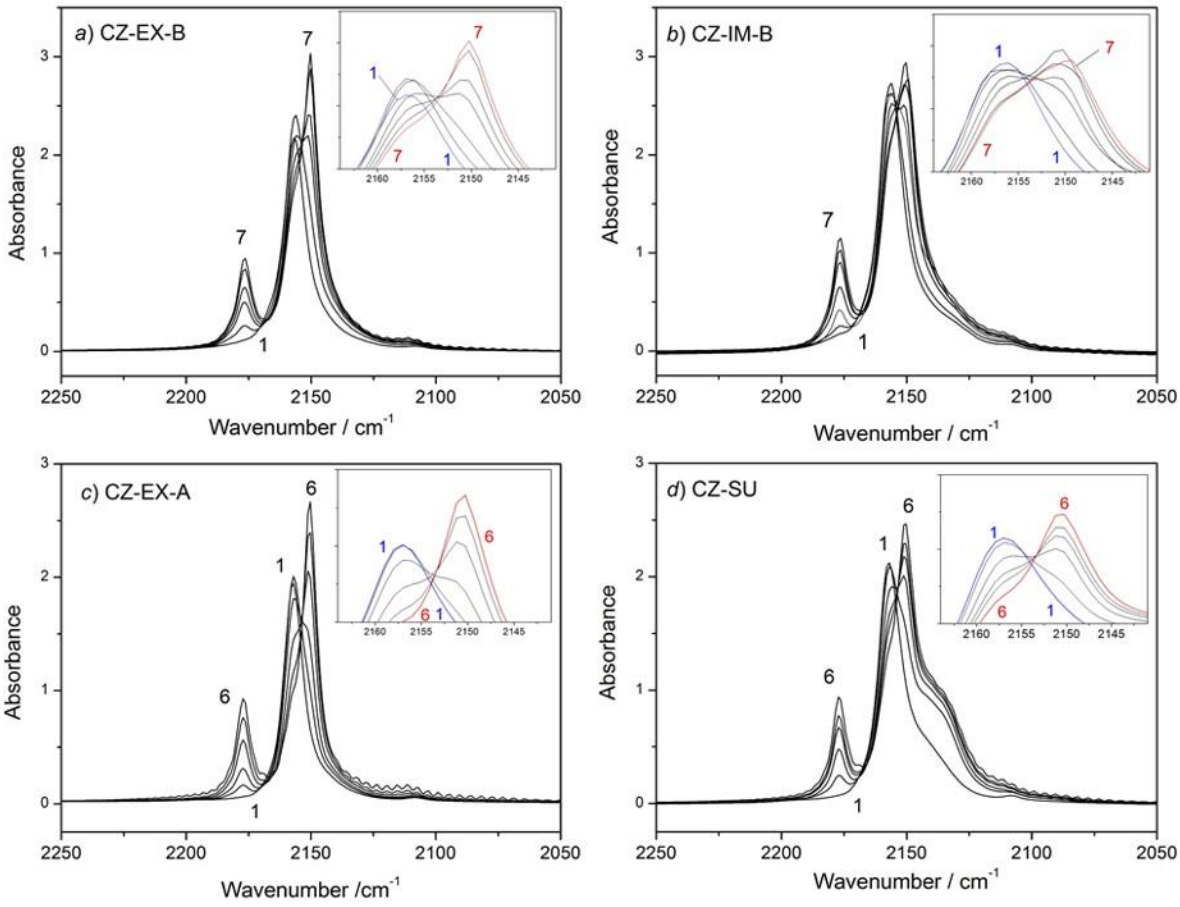

852

853 **Figure 7**

854

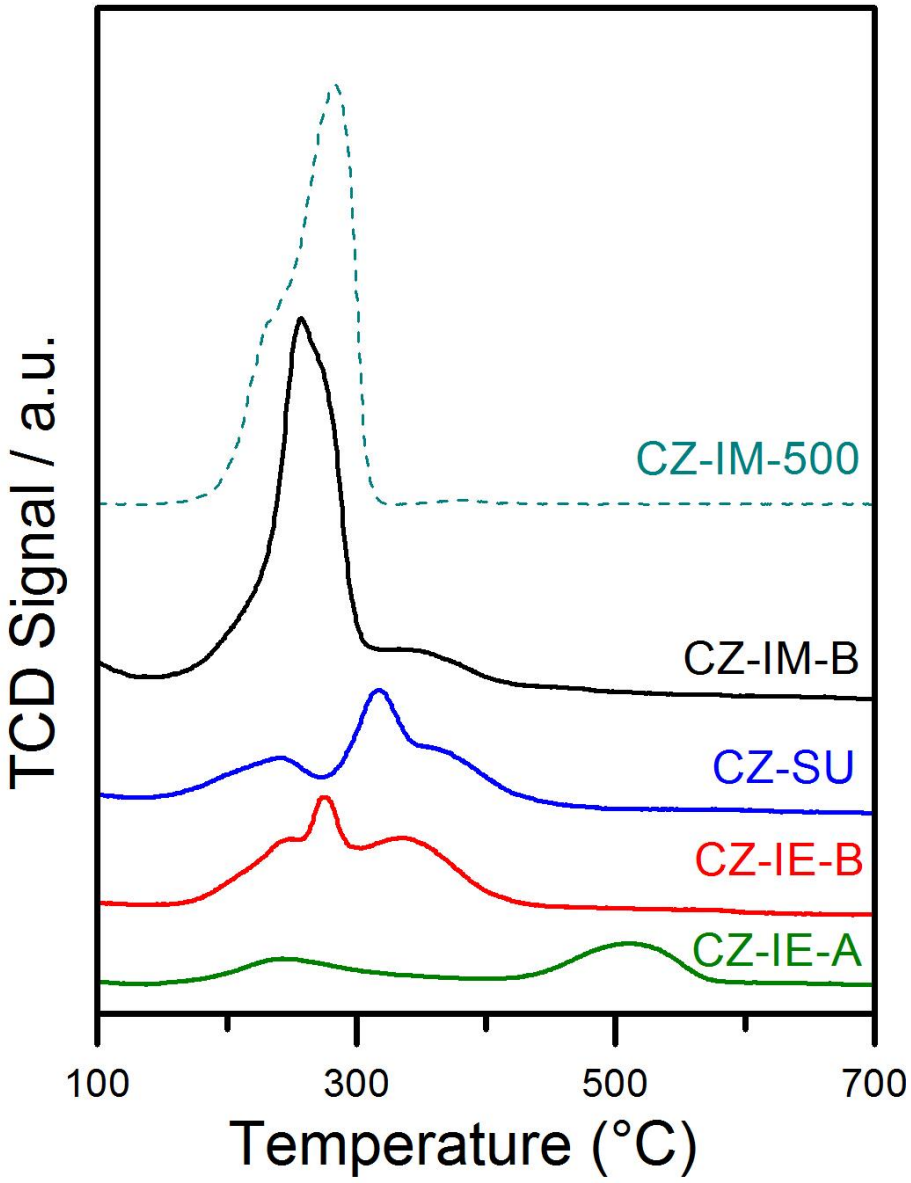

855

856 **Figure 8**